An Effective Image Watermarking System for High Embedding Capacity

Chandan Singh
Professor,
Department of Computer Science
Punjabi University, Patiala

Sukhjeet K. Ranade
Asst. Professor,
Department of Computer Science
Punjabi University, Patiala

ABSTRACT
In this paper, we present a computationally fast and robust image watermarking system with high embedding capacity. The watermark signal is embedded by quantizing the magnitudes of higher order Zernike moments (ZMs). The use of fast and numerically stable method for ZMs computation is proposed to overcome the high computational complexity and numerical instability at the high order of moments. An 8-way symmetry/ anti-symmetry property and recurrence relations for calculation of trigonometric functions are employed to further improve the time and space complexity. Experimental results show that the proposed method provides an excellent tradeoff between embedding capacity, watermark robustness, and visual imperceptibility.

General Terms
Digital image watermarking, Zernike moments.

Keywords
Zernike moments, Embedding capacity, Robustness, Visual imperceptibility, Numerical instability.

1. INTRODUCTION

Digital image watermarking is an effective tool for ensuring copyright protection, content authentication, and integrity verification. A digital watermark is an imperceptible, robust, and secure message embedded in the host image by either directly modifying the bits of image in spatial domain or modifying the coefficients in transform domain [1-3]. In recent years, many low capacity watermarking systems have been developed that perform well against various geometric and common signal processing attacks. Few researchers work on high embedding as increasing capacity adversely affects the visual imperceptibility of watermark and its robustness against various attacks [4]. However, high capacity embedding systems are desirable for variety of applications such as secure media distribution, thumbnail embedding for authentication, and auxiliary data embedding [5]. Another issue that sturdily needs to be addressed while designing an image watermarking system is the computational complexity of embedding and detecting or extracting the watermark from the image. Since most of the digital transmission takes place via Internet, designing an effective watermarking system that can work in limited computing environment can be of immense value for the applications that need to validate the authenticated watermarked images from unauthenticated ones at the router or server itself. This will prevent the circulation of unauthenticated data and nip the evil of digital content piracy.

Various invariant watermarking approaches have been developed in transform domain using Fourier-Mellin transform, discrete Fourier transform, discrete cosine transform, or discrete wavelet transform [6]. Zernike Moments invariants for high capacity image watermarking were first proposed by Farzam and Shirani [7] to embed a watermark that is robust to rotation, noise and JPEG compression. Their method, however, suffered from high computational complexity and sever fidelity loss of watermarked image due to inverse Zernike transform. Later, Kim and Lee [8] proposed a watermarking scheme to embed a zero-bit watermark by modifying the ZMs feature vector consisting of low order ZMs and embedded the watermark signal in spatial domain to avoid fidelity degradation. The first well designed and complete geometrically invariant watermarking scheme using Zernike and pseudo-Zernike moments (ZMs/PZMs) was provably given by Xin et al [9]. In their scheme large data payload is embedded into the feature vector by quantizing the magnitudes of ZMs/PZMs using binary dither modulation. The embedding and reconstruction processes, however, require high order of moments resulting in a huge computational load. More recently, feature based robust watermarking have also been proposed in which some feature-point regions are first selected by using Harris detector [10], Harris-Laplace detector [11] or support vector regression [12] and then the watermark signal is embedded by using the method proposed by Xin et al [9]. However, designing an effective watermark system that allows high embedding capacity remained an unbounded challenge.

Some other moments such as orthogonal moments [13], Krawtchouk moments [14], and Tchebichef moments [15] have also been proposed for invariant image watermarking. But, ZMs are considered superior to other moments because of their immunity to noise, minimum information redundancy, and magnitude invariance property. The magnitude of ZMs is rotation invariant and with some transformations translation and scale invariance can be achieved making them more suitable for geometrically invariant watermarking. However, two major drawbacks related with the usage of ZMs are their high computational complexity and numerical instability at the high order moments. It has been observed that ZMs with order higher than a certain value of $p_{\max}(=44)$ cannot be computed accurately even with the double precision [16]. These limitations are constraint on watermarking system requiring high embedding capacity or limited computing facilities.

In this paper, we propose a fast and efficient high capacity watermarking scheme using fast and numerically stable method for computation of ZMs. An 8-way symmetry/anti-symmetry properties and recurrence relations for the calculation of trigonometric functions are proposed to further optimize the time-space complexity. Image function is normalized with respect to scale and translation before computing the ZMs to achieve complete geometric invariance. Experimental results suggests that the proposed method not only improves the embedding capacity and time complexity of a watermarking system but also enhances the visual imperceptibility and watermark robustness against various

geometric and common signal processing attacks like additive noise, compression, cropping, filtering etc.

Rest of this paper is organized as follows. Section 2 presents an introduction to ZMs. A framework for computationally fast and numerically stable method for calculation of ZMs is given in Section 3. The proposed system for watermark embedding and extraction is outlined in Section 4. Detailed experimental results are given in Section 5 followed by conclusion in Section 6.

2. ZERNIKE MOMENTS

The Zernike moments of order p and repetition q of an image function $f(x,y)$ over a unit disk are defined by

$$A_{pq} = \frac{p+1}{\pi} \iint_{x^2+y^2 \le 1} f(x,y) V_{pq}^{*}(x,y)\, dx\, dy \qquad (1)$$

where image function $f(x,y)$ is defined over a discrete square domain NxN and $V_{pq}^{*}(x,y)$ is the complex conjugate of Zernike polynomial $V_{pq}(x,y)$ given by

$$V_{pq}^{*}(x,y) = R_{pq}(r) e^{-jq\theta} \qquad (2)$$

where

$r = \sqrt{x^2+y^2}$, $j = \sqrt{-1}$, $p \ge 0$, $|q| \le p$, $p - |q| = even$, $\theta = \tan^{-1}(y/x)$, $\theta \in [0, 2\pi]$

and

$R_{pq}(r)$ is the radial polynomial defined as

$$R_{pq}(r) = \sum_{s=0}^{(p-|q|)/2} \frac{(-1)^s (p-s)!\, r^{p-2s}}{s! \left(\frac{p-|q|}{2} - s\right)! \left(\frac{p+|q|}{2} - s\right)!} \qquad (3)$$

Since the exact integration analytical solution of Eq. (1) does not exist, its zeroth order approximation in the discrete domain is given by

$$A_{pq} = \frac{4(p+1)}{\pi N^2} \sum_{i=0}^{N-1} \sum_{\substack{k=0 \\ x_i^2 + y_k^2 \le 1}}^{N-1} f(x_i, y_k) V_{pq}^{*}(x_i, y_k) \qquad (4)$$

where

$$x_i = \frac{2i - N + 1}{N}, \quad y_k = \frac{2k - N + 1}{N}, \quad i,k = 0,1,\ldots,N-1 \qquad (5)$$

One of the major properties of ZMs is that is all moments A_{pq} up to the maximum order of $p_{\max}$ are known, then it is possible to reconstruct the image function using inverse transformation as

$$\hat{f}(x,y) = \sum_{p=0}^{p_{\max}} \sum_{q=-p}^{p} A_{pq} V_{pq}(x,y) \qquad (6)$$

The quality of reconstructed image can be measured using mean square reconstruction error (MSRE) defined as

$$MSRE = \frac{\sum_{i=0}^{N-1} \sum_{k=0}^{N-1} \left[f(x_i, y_k) - \hat{f}(x_i, y_k) \right]^2}{\sum_{i=0}^{N-1} \sum_{k=0}^{N-1} f^2(x_i, y_k)} \qquad (7)$$

3. FAST AND NUMERICALLY STABLE METHOD FOR ZMs COMPUTATION

It can be observed that for an image of size NxN pixels, the time complexity of computing all ZMs up to the maximum order $p_{\max}$ using Eqs. (3) and (4) is $O\left(N^2 p_{\max}^3\right)$, which is very high for large values of N and $p_{\max}$. Numerical instability in the computation of ZMs arises due to two major sources of error namely underflow error (also referred to as overflow) and finite precision error. Many researchers have contributed towards the development of fast and numerically stable methods for ZMs computation [17-19] with fastest method known so far having time complexity $O\left(N^2 p_{\max}^2\right)$. An excellent analysis of time taken and numerical stability for existing methods have been presented by Singh and Walia [20] who have also proposed a computationally fast method for calculation of ZMs at high order of moments. Their method optimizes the speed of *modified Kintner's method* [19] by redefining some of the coefficients required in the computation of recurrence relations. This method known as *modified Kintner's fast method* is summarized as follows.

Evaluate the following for $q = 0,1,2,\ldots,p_{\max}$ for the given maximum order of moments $p_{\max}$

$$R_{qq}(r) = r^q, \; q = 0,1,2\ldots, p_{\max} \qquad (8)$$

$$R_{pq}(r) = pR_{pp}(r) - (p-1)R_{p-2,p-2}(r), \; q = 0,1,2,\ldots, p_{\max} - 2 \quad (p = q+2) \qquad (9)$$

$$R_{pq}(r) = (K_2' r^2 + K_3') R_{p-2,q}(r) + K_4' R_{p-4,q}(r), \quad p = q+4, q+6, \ldots, p_{\max} \qquad (10)$$

where

$$K_2' = K_2/K_1, \; K_3' = K_3/K_1, \; K_4' = K_4/K_1 \qquad (11)$$

and

$$K_1 = \frac{(p+q)(p-q)(p-2)}{2} \qquad (12)$$

$$K_2 = 2p(p-1)(p-2) \qquad (13)$$

$$K_3 = -q^2(p-1) - p(p-1)(p-2) \qquad (14)$$

$$K_4 = \frac{-p(p+q-2)(p-q-2)}{2} \qquad (15)$$

3.1 Recurrence Relation for Computation of Trigonometric Functions

To further speed up the computation of ZMs we propose following recurrence relations for the evaluation of trigonometric functions at each pixel position (x_i, y_k) for $q = 0,1,\ldots,p_{\max}$ and save them in two tables $C[q]$ and $S[q]$.

- *Initialize*

  $r = sqrt(x_i^2 + y_k^2)$, $C[0] = 1$, $S[0] = 0$,

  $C[1] = x_i/r$, $S[1] = y_k/r$, $T = 2 \cdot C[1]$

- *for* $q = 1$ *to* $p_{\max} - 1$

$$C[q+1] = C[q].T - C[q-1]$$
$$S[q+1] = S[q].T - S[q-1]$$

The above recursive method improves the speed of computation at the additional requirement of only $2(p_{\max}+1)$ memory words used for saving values of sine and cosine functions.

3.2 An 8-way Symmetry/Anti Symmetry Property

Recently, Singh and Walia [21] proposed the use of symmetry/ anti-symmetry property for computation of trigonometric functions in radial polynomial. If $P(x_i, y_k)$ is an image pixel at location (i,k), then the value of radial polynomial $R_{pq}(r)$ is same for pixels at locations $(\pm x_i, \pm y_k)$ and $(\pm y_k, \pm x_i)$. Thus, we need to compute trigonometric functions $\cos(q\theta_{ik})$ and $\sin(q\theta_{ik})$ only in the first octant and values at seven other locations, $n\pi/2 \pm \theta_{ik}$ $n = 1,2,3,4$ ($2\pi + \theta_{ik}$ is discarded) can be obtained by using periodicity of sinusoidal functions. An 8-way symmetry/anti symmetry property reduces the number of computations and space complexity required for trigonometric functions from N^2 to $N(N+1)/8$.

4. PROPOSED WATERMARKING SYSTEM

Based on computation method presented in Section 3 we design an efficient and high capacity image watermarking scheme robust against geometric and other common signal processing attacks. An array of bits is embedded by quantizing the magnitudes of selected ZMs through quantization index modulation [9]. For watermark extraction the selected ZMs are re-quantized from possibly manipulated image and array of bits is retrieved by using a minimum distance decoder with possibly low error rate. Various steps required for watermark embedding and extraction are summarized as follows.

(i) Watermark bit sequence: Our watermark bit sequence $B = \{b_i, i = 1,2,\ldots,L\}$ consists of L number of information bits such that $b_i \in \{0,1\}$.

(ii) Image normalization: Image normalization is performed to achieve translation and scale invariance. An image function $f(x,y)$ can be normalized by transforming it into $g(x,y)$, where

$$g(x,y) = f\left(\frac{x}{a} + \bar{x}, \frac{y}{a} + \bar{y}\right) \qquad (16)$$

with $(\bar{x}, \bar{y})$ being the centroid of $f(x,y)$ and $a = \sqrt{\beta / m_{00}}$, with β a predetermined value and m_{00} its zeroth-order moment [8].

(iii) Selection of ZMs: As analyzed by Xin et al [9], all moments with repetition $q = 4i$, i integer, cannot be computed accurately and are not suitable for watermark embedding. Therefore, the set of applicable ZMs can be denoted by $S = \{Z_{pq}, p \le p_{\max}, q \ge 0, q \ne 4i\}$ and the cardinality of S is given by

$$|S| = \begin{cases} \dfrac{3p_{\max}^2 + 8p_{\max}}{16} & if\ p_{\max} = 4i \\ \dfrac{3p_{\max}^2 + 10p_{\max} + 3}{16} & if\ p_{\max} = 4i+1 \\ \dfrac{3p_{\max}^2 + 8p_{\max} + 4}{16} & if\ p_{\max} = 4i+2 \\ \dfrac{3p_{\max}^2 + 10p_{\max} + 7}{16} & if\ p_{\max} = 4i+3 \end{cases} \qquad (17)$$

where i is any nonnegative integer and $p_{\max}$ is the maximum order of ZMs that determines the embedding capacity of watermarking system.

(iv) Quantization of ZMs: Depending on the length of watermark bit sequence, $L \le |S|$, a number of ZMs are selected to form the ZMs feature vector $Z = \{Z_{p_1,q_1}, Z_{p_2,q_2}, \ldots, Z_{p_L,q_L}\}$. Each bit b_i from B is embedded into the corresponding element Z_{p_i,q_i} of Z to obtain modified ZMs feature vector $\tilde{Z} = \{|\tilde{Z}_{p_1,q_1}|, |\tilde{Z}_{p_2,q_2}|, \ldots, |\tilde{Z}_{p_L,q_L}|\}$ by using dither modulation and $|\tilde{Z}_{p_i,q_i}|$ is the quantized version of $|Z_{p_i,q_i}|$ computed as follows.

$$|\tilde{Z}_{p_i,q_i}| = \left[\frac{|Z_{p_i,q_i}| - d_i(b_i)}{\Delta}\right]\Delta + d_i(b_i), \quad i = 1,2,\ldots,L \qquad (18)$$

where, $[.]$ denotes the rounding operation, Δ is the step size of quantization and $d_i(.)$ is the dither value for the ith quantizer with constraint $d_i(1) = d_i(0) + \Delta/2$. The dither vector $(d_1(0), d_2(0), \ldots, d_L(0))$ whose elements are uniformly distributed over $[0, \Delta/2]$, is pseudo randomly generated using seed *K* to facilitate the process of extraction and further enhance the security of embedding. The modified ZMs can now be computed as

$$\tilde{Z}_{p_i,q_i} = \frac{|\tilde{Z}_{p_i,q_i}|}{|Z_{p_i,q_i}|} Z_{p_i,q_i}, \quad i = 1,2,\ldots,L \qquad (19)$$

While quantizing, $\tilde{Z}_{p_i,q_i}$, if $q_i \ne 0$, then its complex conjugate $\tilde{Z}_{p_i,-q_i}$ is also quantized to ensure that they always have the same magnitudes.

(v) Formation of watermarked image: After modifying the selected ZMs, the spatial watermark signal, $w(x,y)$, is reconstructing using Eq. (6) as follows.

$$w(x,y) = \sum_{i=1}^{L} \left[\varepsilon_{p_i,q_i} V_{p_i,q_i}(.) + \varepsilon_{p_i,-q_i} V_{p_i,-q_i}(.)\right] \qquad (20)$$

where $\varepsilon_{p_i,q_i} = \tilde{Z}_{p_i,q_i} - Z_{p_i,q_i}$ and $\varepsilon_{p_i,-q_i} = \tilde{Z}_{p_i,-q_i} - Z_{p_i,-q_i}$, $i = 1,2,\ldots,L$. The final watermarked image $f_{wat}(x,y)$ is formed as

$$f_{wat}(x,y) = f(x,y) + w(x,y) \qquad (21)$$

(vi)Watermark extraction: The watermark extraction process tries to get an estimate of embedded sequence

$\hat{b} = (\hat{b}_1, \hat{b}_2, \ldots, \hat{b}_L)$ from the received image $f'_{wat}(x, y)$ which may be distorted version of $f_{wat}(x, y)$ with possibly low error rate. The process of extraction is similar to the embedding process. First, the relevant ZMs feature vector $Z' = \{Z'_{p_1,q_1}, Z'_{p_2,q_2}, \ldots, Z'_{p_L,q_l}\}$ is computed from the received image after normalization and then reusing Eq. (18), magnitude of each Z'_{p_i,q_i} is re-quantized with both dither functions $d_i(0)$ and $d_i(1)$ to compute $\left|Z'_{p_i,q_i}\right|_0$ and $\left|Z'_{p_i,q_i}\right|_1$, respectively. A minimum distance decoder is used to estimate the bit embedded in Z'_{p_i,q_i} as follows.

$$\hat{b}_i = \arg\min_{j\in\{0,1\}} \left(\left|Z'_{p_i q_i}\right|_j - \left|Z'_{p_i q_i}\right| \right)^2, \; i = 1,2,\ldots,L \qquad (22)$$

5. EXPERIMENTAL RESULTS

We performed numerous experiments to analyze the embedding capacity, visual imperceptibility, robustness, and time complexity of proposed watermarking algorithm. A 512-bit randomly generated watermark signal was embedded into gray scale image of size 256x256 pixels with maximum order of moments $p_{\max} = 55$. Fig. 1(a)-(c) shows the sample original image, the watermarked image, and spatial watermark signal magnified 10 times for better display.

(a) **(b)** **(c)**

Fig. 1: Example of watermark embedding (a) sample test image Lena (b) the output watermarked image ($p_{\max} = 55, \Delta = 1.0, L = 512, PSNR = 51.87\ dB$) (c) spatial watermark signal

5.1 High Embedding Capacity

It has been pointed out [16] that the traditional zeroth order approximation method provides accuracy only for the values of $p_{\max} \le 44$ limiting maximum embedding capacity up to 385 bits or approximately 48 characters. The accuracy and robustness of a watermarking system is measured quantitatively using bit error rate (BER). Defined as ratio of number of bits extracted inaccurately to total number of bits embedded, the value of BER lies between 0 and 1 with $BER \ge 0.25$ indicating failure to extract the watermark. We embedded randomly generated watermark of varying length L computed using Eq. (17) for $p_{\max} \le 100$ and plotted the BER curves obtained after extracting watermark sequence from un-attacked watermarked image using traditional method and the proposed method. As shown in Fig. 2, performances of two methods are comparable for watermark length L less than 385 or $p_{\max} \le 44$. The traditional method fails to extract the watermark $(BER \ge 0.25)$ for $L > 385$ as ZMs magnitudes become highly instable at higher order of moments. It must be noted that average $BER \approx 0.5$ is obtained with traditional method as statistically about 50% of the bits extracted turned out to be correct due to random behavior whereas the proposed method provides excellent accuracy at higher embedding strengths of $L \ge 1000$. The maximum BER obtained is 0.037 which is very small and within acceptable limits.

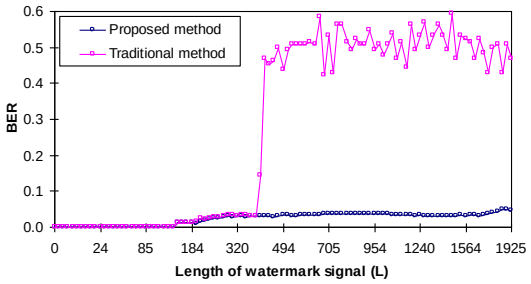

Fig. 2: BER vs. number of bits embedded with order of moments $p_{\max} \le 100$

5.2 Quality of Watermarked Images

One of the major challenges while designing a high capacity watermark system is its adverse affect on visual imperceptibility and robustness of watermark. The visual imperceptibility of watermarked image $f_{wat}(x, y)$ with respect to the original input image $f(x, y)$ is measured quantitatively using peak-signal-to-noise-ratio (PSNR) defined as

$$PSNR(f, f_{wat}) = 10\log_{10}\left(\frac{255^2 \times N^2}{\sum_{i=1}^{N}\sum_{k=1}^{N}\left[f_{wat}(x_i, y_k) - f(x_i, y_k)\right]^2} \right) \qquad (23)$$

The quantization step Δ determines embedding strength or watermark robustness with higher values of Δ ensuring better robustness. We computed the PSNR for values of Δ from 0.8 to 2.0 after embedding three watermark sequences of length 256-, 512- and 1024- bits. It can be observed from Fig. 3 that the proposed method provides good visual imperceptibility with value of $PSNR \ge 44dB$. For all our further experiments we chose quantization step $\Delta = 1.0$ to ensure good visual imperceptibility.

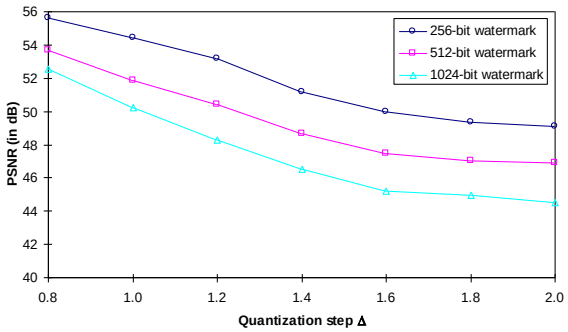

Fig. 3: Visual imperceptibility of watermark for varying values of quantization step Δ and bits embedded

5.3 Robustness of the Proposed Method

We measured the robustness of proposed watermarked system under various attacks and plotted the BER curves after embedding 256 and 512-bit random sequences with order of moments $p_{\max} = 60$. Each of the data point in graphs

presented in this section represents the average BER value of 100 test cases.

5.3.1 Robustness to image rotation

In our experiments, forty-five different rotation angles from 0 to 45^o were tried with an interval of 1^o. The watermarked image of size 256x256 pixels was rotated using inverse rotation transformation for better pixel sampling [16]. Fig. 4 shows the results for embedding 256 and 512 bits. It can be observed from the figure that the proposed method provides god robustness against the rotation attack even for higher embedding strengths.

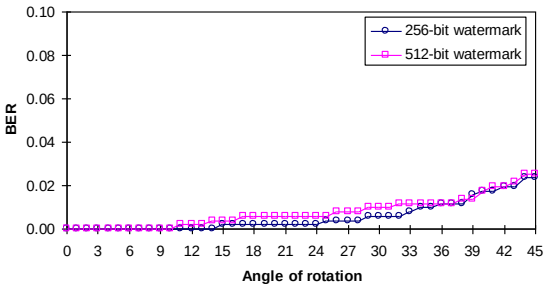

Fig. 4: Watermark robustness to rotation

5.3.2 Robustness to image scaling

The watermarked image of standard size 256x256 pixels is scaled with fourteen different scaling factors ranging from 0.0125 to 2.0 using bi-linear interpolation. No re-scaling was required prior to watermark extraction as image normalization provides magnitude invariance against scaling. Fig. 5 shows the BER curves after embedding 256 and 512-bit sequences. As shown in the figure our proposed method provides comparable robustness even for greater embedding strength under all scaling factors. We obtained zero bit error when watermarked images are scaled to sizes larger than standard size as there is no loss of information during the interpolation process.

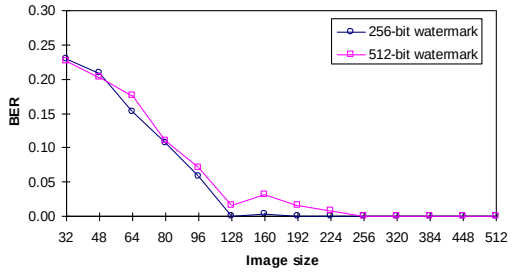

Fig. 5: Watermark robustness to scaling

5.3.3 Robustness to image compression

JPEG compression is one of the commonly used lossy image compression technique. We examined the BER for JPEG compression with twelve different quality factors ranging from 15 to 100. Fig. 6 shows the average BER curves of 100 test cases obtained after embedding 256 and 512-bit randomly generated watermark sequence. It can be seen from the figure that the proposed method provide excellent performance even for poor JPEG quality factors and higher embedding strengths.

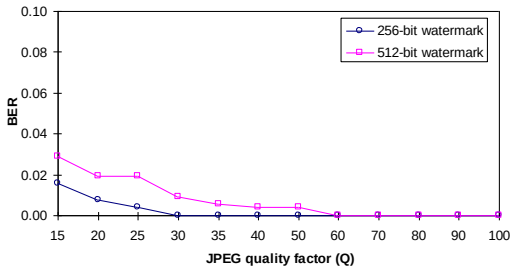

Fig. 6: Watermark robustness to JPEG compression

5.3.4 Robustness to additive noise

Additive uniform noise models most of the common interferences watermarked images may undergo. Fig. 7 shows the average BER values for different levels of uniform noise ranging from zero to 100 percent for 256 and 512-bit watermarks. The proposed method provides excellent robustness to additive noise up to 50%. In fact, the additive noise higher than 50% causes much degradation to quality of image and is unlikely to occur; we can conclude that the proposed method is robust to additive noise for higher embedding strengths.

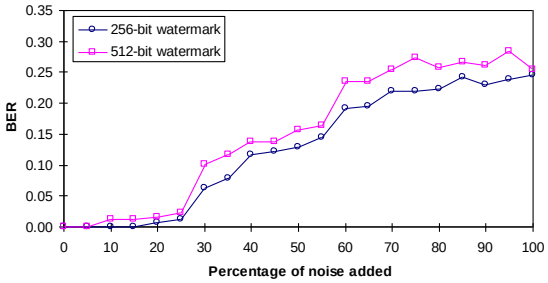

Fig. 7: Watermark robustness to additive noise

5.3.5 Robustness to Stirmark attacks

We examined the robustness of watermarked image to some common Stirmark attacks [22] like cropping, filtering, affine transformation etc. A 512-bit randomly generated sequence was embedded to the host image of size 256x256 pixels and various attacks were performed by Stirmark 4.0 tool. The average BER of ten test images is listed in Table 1. It can be observed from the table that the proposed method is found completely robust in case of cropping less than 10%, JPEG quality factor above 50, median filter of window size 3x3, rescaling ≥100%, rotations at $\pm 90^o$ and flipping with average $BER = 0$ and provides good robustness against minor affine transformations, cropping $\geq 20\%$, JPEG compression, scaling, and rotation.

Table 1 Stirmark test results

Attack	Average BER
Shearing *x*:0.05 *y*:0.00	0.0854
Shearing *x*:0.00 *y*:0.05	0.0763
Cropping <10%	0
Cropping 10-20%	0.0307
JPEG quality <25	0.0025
JPEG quality 25-50	0.0007
JPEG quality >50	0
Median Filter 3x3	0
Median Filter 5x5	0.0070
Rescaling <50%	0.0218
Rescaling 50-75%	0.0031
Rescaling ≥ 100%	0
Rotation ±0.25	0.0152
Rotation ±0.50	0.0300
Rotation ±0.75	0.0354
Rotation ± 90.00 and Flipping	0

5.4 Time Complexity of Proposed Method

Time complexity is another important issue we identify with the performance of watermarking system. The time complexity of proposed *modified Kintner's fast method* for computing all ZMs up to the maximum order $p_{\max}$ is $O\left(N^2 p_{\max}^2\right)$. We compared the speed of the proposed and traditional methods in terms of average time taken for watermark embedding. Both methods are implemented in VC++ 6.0 under Windows-XP environment on Intel 1.60 GHz processor with 1GB RAM. Fig. 8 shows the curves depicting the time taken for embedding total number of bits given by Eq. (17) up to maximum order of moments $p_{\max} \le 36$ in a gray scale host image of size 128x128 pixels. The weighted averages for the proposed and traditional method for ZMs computations are 0.167 seconds, and 1.615 seconds, respectively indicating considerable improvement in time complexity by the proposed method.

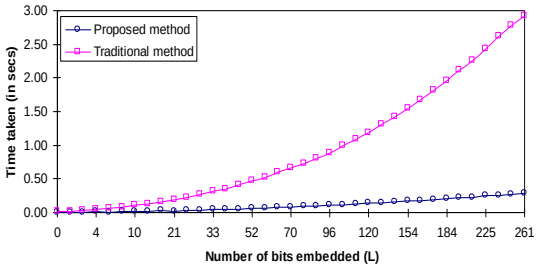

Fig. 8: Comparison of embedding speed

6. CONCLUSION

We have developed an effective image watermarking algorithm for high capacity data embedding using fast and numerically stable method of ZMs computation. The proposed method uses *modified Kintner's fast method* for ZMs computation because it is more accurate and numerically stable at higher order of moments. An 8-way symmetry/anti-symmetry property and recurrence relations for calculation of trigonometric functions are proposed to further enhance the time-space complexity of watermarking system. Image normalization is performed to achieve magnitude invariance of ZMs against all kind of geometric distortions. It has been observed that the proposed method provide high data embedding capacity and reduced computational cost without sacrificing the robustness and perceptual quality of watermarked images. Hence, the proposed method is very effective for watermark system requiring high embedding capacity and limited computation facilities.

7. REFERENCES

[1] Cox, I.J., Kilian, J., Leighton, F.T., and Shamoon, T. 1997. Secure Spread Spectrum Watermarking for Multimedia. IEEE Transactions on Image Processing 6(12):1673-1687.

[2] O' Ruanaidh, J.J.K. and Pun, T. 1998. Rotation, Scale and Translation Invariant Spread Spectrum Digital Image Watermarking. Signal Processing. 66(8):pp. 303-317.

[3] Petitcolas, F.A.P., Anderson, R.J., and Kuhn, M.G. 1999. Information Hiding| A Survey. In proceedings of the IEEE Special issue on Protection of Multimedia content. 87(7):1062-1078

[4] Lan, T.-H. and Tewfik A.H. 2006. A Novel High-Capacity Data-Embedding System. IEEE Transactions on Image Processing, 15(8):2431-2440.

[5] Kumar, P.M. and Shunmuganathan, K.L. 2010. A reversible high embedding data hiding technique for hiding secret data in images. International Journal of Comp. Sci. and Inf. Security 7(3): 109-115

[6] Potdar, V. M., Han, S. and Chang, E. 2005. A Survey of Digital Image Watermarking Techniques. In proceedings of 3rd IEEE International Conference on Industrial Informatics. INDIN: 709-716.

[7] Farzam, M. and Shirani, S. 2001. A Robust Multimedia Watermarking Technique using Zernike Transform. IEEE 4th Workshop on Multimedia Signal Processing. 529-534

[8] Kim, H.S., and Lee, H.-K. 2003. Invariant Image Watermark using Zernike Moments. IEEE Transactions on Circuits and Systems for Video Tech. 13(8): 766-775.

[9] Xin, Y., Liao, S. and Pawlak, M. 2007 Circularly Orthogonal Moments for Geometrically Robust Image Watermarking, Pattern Recognition 40: 3740-3752.

[10] Singhal, N., Lee, Y.-Y., Kim, C.-S. and Lee, S.-U. 2009. Robust Image Watermarking using Local Zernike Moments. Journal of Vision Communication and Image Representation 20:408-419.

[11] Wang, X.-Y., Hou, L.-M. and Yang, H.-Y. 2009. A Feature-Based Image Watermarking Scheme Robust to Local Geometrical Distortions. Journal of Optics A: Pure and Applied Optics. DOI:10.1088/1464-4258/11/6/065401

[12] Wang, X.-Y., Xu, Z.-H., and Yang, H.-Y. 2009. A Robust Image Watermarking Algorithm using SVR Detection. Expert Systems with Applications. 36:9056-9064.

[13] Yap, P.-T. and Paramesran, R. 2005. An Image Watermarking Scheme Based on Orthogonal Moments.

In proceedings of TENCON. IEEE Region 10 Conference.

[14] Venkataramana, A. and Raj, P. A. 2007. Image Watermarking using Krawtchouk Moments. In proceedings of the IEEE International Conference on Computing: Theory and Applications.

[15] Deng, C. Gao, X., Li, X. and Tao, D. 2009. A local Tchebichef moments-based robust image watermarking. Signal Processing 89:1531-1539.

[16] Singh, C. 2006. Improved quality of Reconstructed Images using floating point arithmetic for moment calculation. Pattern Recognition. 39:2047-2064.

[17] Kintner, E.C. 1976. A Recursive Relation for Calculating the Zernike polynomials. Opt. Acta 23 (6):489-500.

[18] Prata, A. and Rusch, W.V.T. 1989. Algorithm for computation of Zernike polynomials expansion coefficients. Appl. Opt. 28:749-754.

[19] Chong, C.-W., Paramesran, R. and Mukundan, R. 2003. A comparative analysis of algorithms for fast computation of Zernike moments. Pattern Recognition. 36:731-742

[20] Singh, C. and Walia, E. 2010. Fast and Numerically Stable Methods for the Computation of Zernike moments. Pattern Recognition. 43: 2497-2506.

[21] Singh, C. and Walia, E. 2011. Algorithms for Fast Computation of Zernike moments and their Numerical Stability. Image and Vision Computing. 29:251-259

[22] Petitcolas, F.A.P., Steinebach, M., Raynal, F., Dittmann, J., Fontaine, C. and Fates, N. 2001. A public automated web-based evaluation service for watermarking schemes: StirMark Benchmark. In proc. of SPIE. 4314: 575- 584